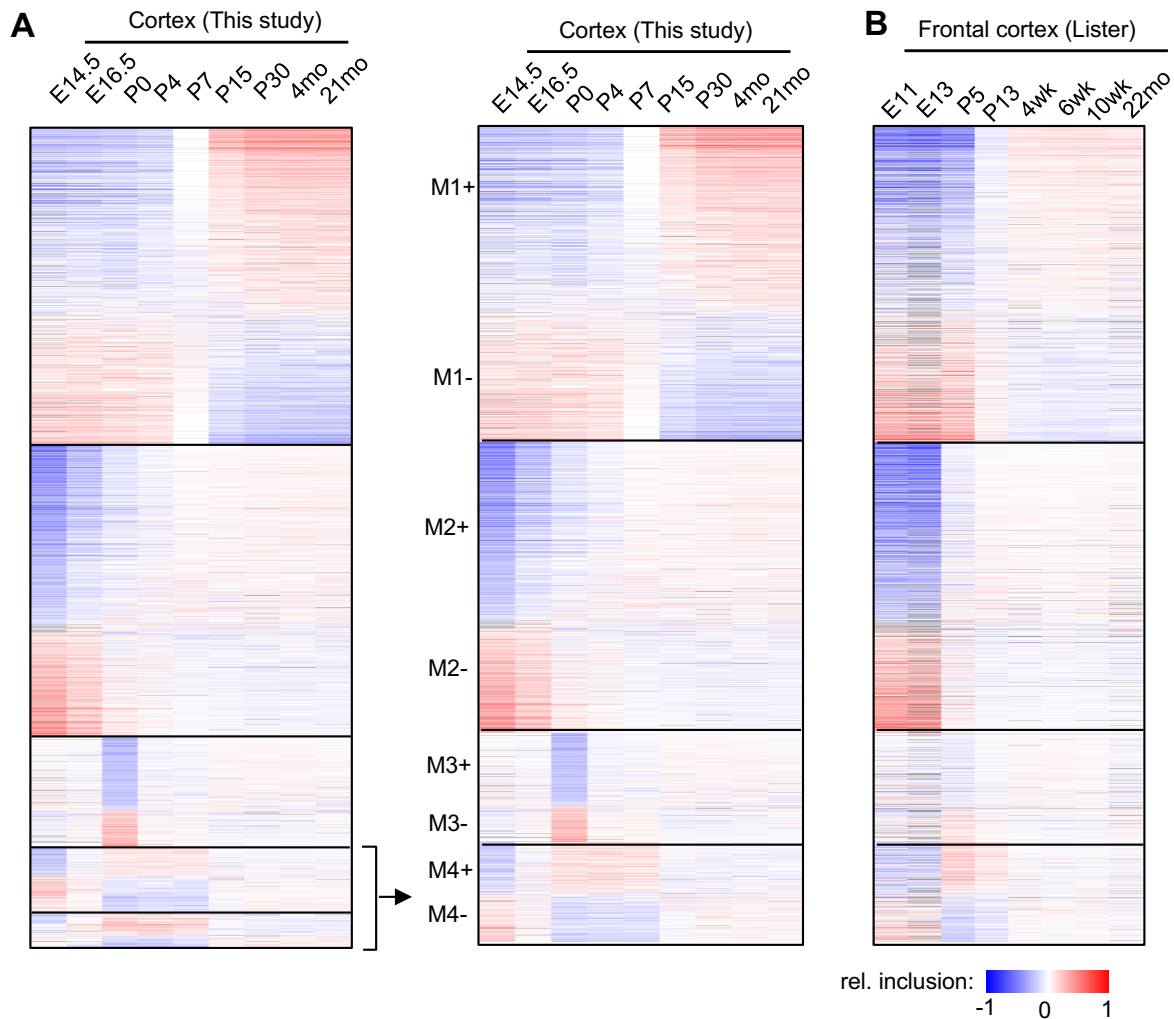
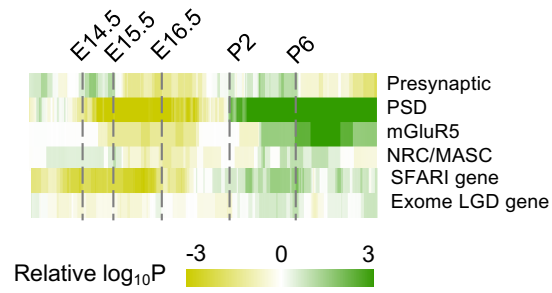


**Fig. S1. Validation of developing cortex RNA-seq data and AS quantification.** (A) Pairwise correlation of gene expression in mouse cortices between different developmental stages. Duplicates were analyzed at each time point. (B) Similar to (A), but pairwise correlation estimated from inclusion level of ~16,000 known cassette exons. (C) *Mapt* exon 10 as an example of developmentally regulated exons. (D) Semi-quantitative RT-PCR validation of splicing for *Mapt* exon 10 in the cortex and cerebellum. (E) A summary of splicing quantification of 10 exons at different developmental stages using RT-PCR and RNA-seq.



**Fig. S2. Robustness of the modular organization of developmentally regulated alternative exons in an independent dataset.** (A) Related to Fig. 1D in the main text, WGCNA initially identified five modules. Modules 4 and 5, together composed of 353 of 2,883 exons, both capture non-monotonic splicing changes with similar temporal patterns and were merged manually into a final module M4 presented in the paper. (B) Comparison of splicing in an independent dataset derived from mouse frontal cortices at different developmental stages from E11 to adult. Exons are shown in the same order as in the right panel in (A). Exons in three of the four modules (M1, M2, and M4) show very similar developmental switches. Since P0 was not included in this second dataset, the reproducibility of the distinct splicing pattern of exons in module M3 could not be evaluated here (however, this module is reproducible in other datasets that include P0 or P1, see e.g., Fig. 2A in the main text). Note that the denser sampling of time points before P15 in our cortex RNA-seq dataset allows us to capture more dynamics.



**Fig. S3. Functional enrichment of genes with splicing switches with specific timing.** Related to Fig. 1E in the main text, exons were ranked based on the timing of splicing switches. Exons in each sliding window (with a window size of 300 exons) were compared to all cassette exons with sufficient read coverage in the cortex to evaluate enrichment of genes with specific functional annotations (see Materials and Methods).

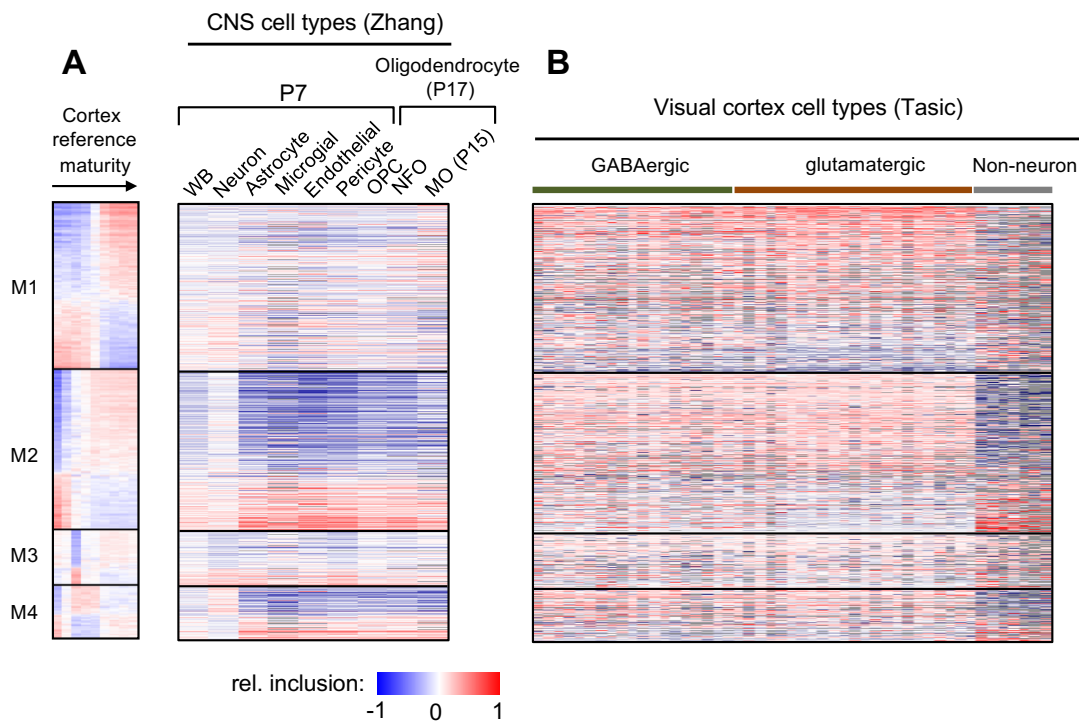


**Fig. S4. The splicing profile of different cell types in the cortex.** Related to Fig. 2 in the main text, splicing profiles of module exons are shown for different cell types isolated from the cortex. In each panel, exons are shown in the same order as in the cortex reference on the left. **(A)** In the Zhang et al. dataset, oligodendrocyte progenitor cells (OPCs), newly formed oligodendrocyte (NFO) and myelinated oligodendrocytes (MO) were purified from P17 mice, while the remaining samples were purified from P7 mice. **(B)** The Tasic et al. dataset are single-cell RNA-seq profiles from the primary visual cortex of adult mice. In this dataset, splicing profiles were quantified by pulling reads from cells that are core members of each cell type. Specific subtypes were ordered based on the broad categories (GABAergic interneurons, glutamatergic pyramidal neurons, and non-neuronal cell types).

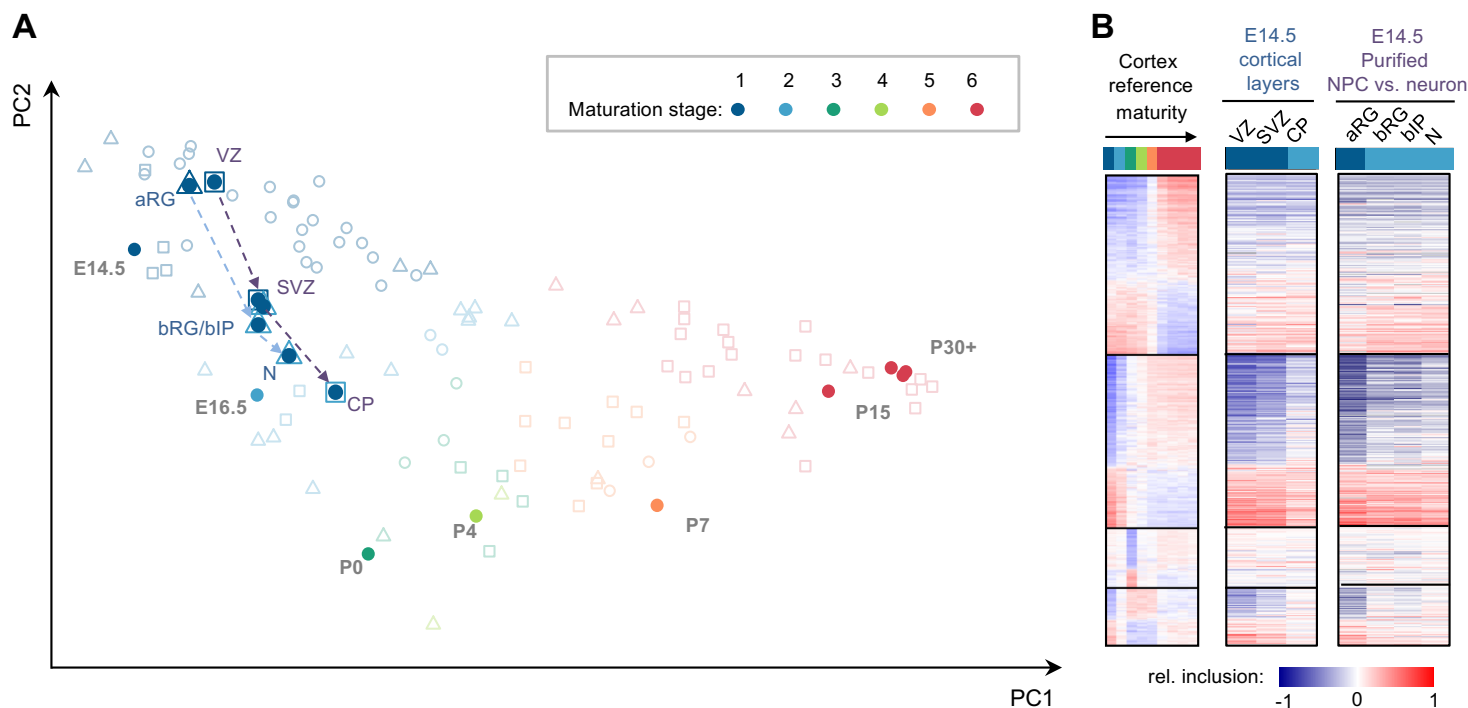


**Fig. S5. Different subpopulations of cells in germinal zones of embryonic cortex show different stages of maturation. (A)** Related to Fig. 2B in the main text, but samples from different germinal zones or different cell populations purified from embryonic cortex are labeled. VZ: ventricular zone; SVZ: sub-ventricular zone; CP: cortical plate; aRG: apical radial glial cells; bRG: basal radial glial cells; bIP: basal intermediate progenitor cells; N: neurons. Note that while the correct stage (stage 1) was assigned to samples from the VZ or SVZ-IZ, which are enriched in progenitor cells, a more mature stage (stage 2) was assigned to CP samples enriched in post-mitotic neurons, which is consistent with the pattern of neuron migration and maturation during cortical development; similar classification inaccuracies were made for late-stage radial glial cells and neurons FACS-purified from the embryonic cortex. **(B)** Splicing profiles of module exons are shown for samples labelled in panel (A).



**Fig. S6. *De novo* motif analysis on WGCNA module exons.** Core exons in modules M1 and M2 in each direction were compared with all mouse cassette exons to evaluate the enrichment of each hexamer in the upstream and downstream intronic sequences (200 nt on each side). Only the top 20 words are shown and hexamers that resemble consensus binding sites of known RBPs are indicated. Motif enrichment in the alternative exon is also evaluated but no significant hexamers were found.

| UI3 (200 nt)   |             |             |                 |     | DI5 (200 nt) |             |                 |
|----------------|-------------|-------------|-----------------|-----|--------------|-------------|-----------------|
| Motif          | fg          | log2FC      | pval            |     | fg           | log2FC      | pval            |
| TCTY (Ptpb)    | <b>1219</b> | <b>0.30</b> | <b>7.40E-13</b> | M1+ | 891          | 0.11        | 1.03E-02        |
| YCAY (Nova)    | 1085        | 0.10        | 9.46E-03        |     | 1097         | 0.11        | 5.49E-03        |
| TGCATG (Rbfox) | 33          | 0.36        | 9.50E-02        |     | <b>80</b>    | <b>1.34</b> | <b>8.41E-13</b> |
| YGCY (Mbnl)    | 876         | 0.06        | 1.17E-01        |     | <b>1271</b>  | <b>0.59</b> | <b>3.72E-42</b> |
| TCTY (Ptpb)    | 689         | 0.11        | 2.70E-02        | M1- | 532          | 0.10        | 6.76E-02        |
| YCAY (Nova)    | 704         | 0.11        | 2.08E-02        |     | 690          | 0.17        | 1.22E-03        |
| TGCATG (Rbfox) | 27          | 0.71        | 1.15E-02        |     | 31           | 0.66        | 1.08E-02        |
| YGCY (Mbnl)    | <b>733</b>  | <b>0.44</b> | <b>1.94E-15</b> |     | 587          | 0.19        | 1.09E-03        |
| TCTY (Ptpb)    | <b>1392</b> | <b>0.48</b> | <b>1.64E-32</b> | M2+ | 864          | 0.11        | 1.72E-02        |
| YCAY (Nova)    | 1020        | 0.00        | 5.33E-01        |     | <b>1233</b>  | <b>0.32</b> | <b>2.14E-14</b> |
| TGCATG (Rbfox) | 34          | 0.39        | 7.62E-02        |     | <b>88</b>    | <b>1.53</b> | <b>6.62E-17</b> |
| YGCY (Mbnl)    | 1079        | 0.35        | 1.13E-14        |     | 1069         | 0.37        | 8.21E-16        |
| TCTY (Ptpb)    | 504         | -0.01       | 5.67E-01        | M2- | 437          | 0.10        | 8.45E-02        |
| YCAY (Nova)    | <b>664</b>  | <b>0.37</b> | <b>1.63E-10</b> |     | 534          | 0.08        | 9.17E-02        |
| TGCATG (Rbfox) | <b>25</b>   | <b>0.94</b> | <b>2.29E-03</b> |     | 17           | 0.07        | 4.52E-01        |
| YGCY (Mbnl)    | 479         | 0.16        | 1.01E-02        |     | 453          | 0.10        | 7.98E-02        |

**Fig. S7. Consensus motif analysis on WGCNA module exons.** Core exons in modules M1 and M2 in each direction were compared with all mouse cassette exons to evaluate the enrichment of the consensus motif for Nova, Rbfox, Mbnl and Ptpb in the upstream and downstream intronic sequences (200 nt on each side).



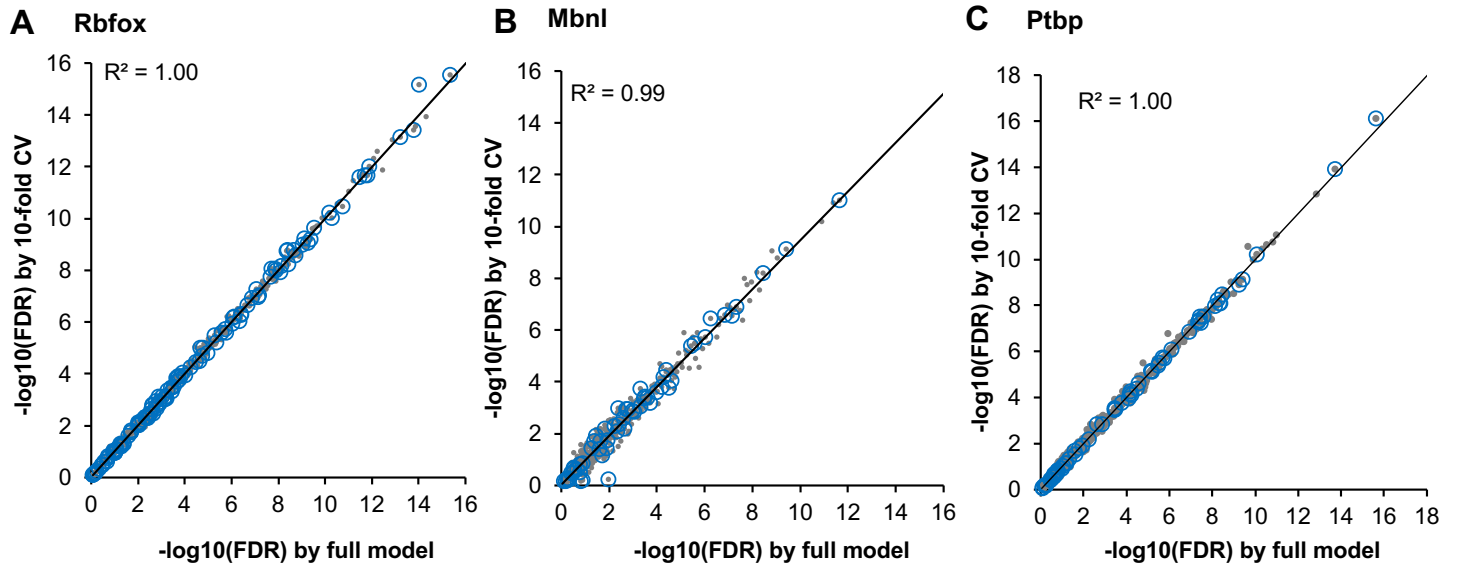


**Fig. S8. 10-fold cross validation of Bayesian network analysis to predict RBP target exons. (A)** Rbfox. **(B)** Mbni. **(C)** Ptbp. In each panel, exons used for model training and cross validation are shown. Previously validated exons are highlighted in blue.

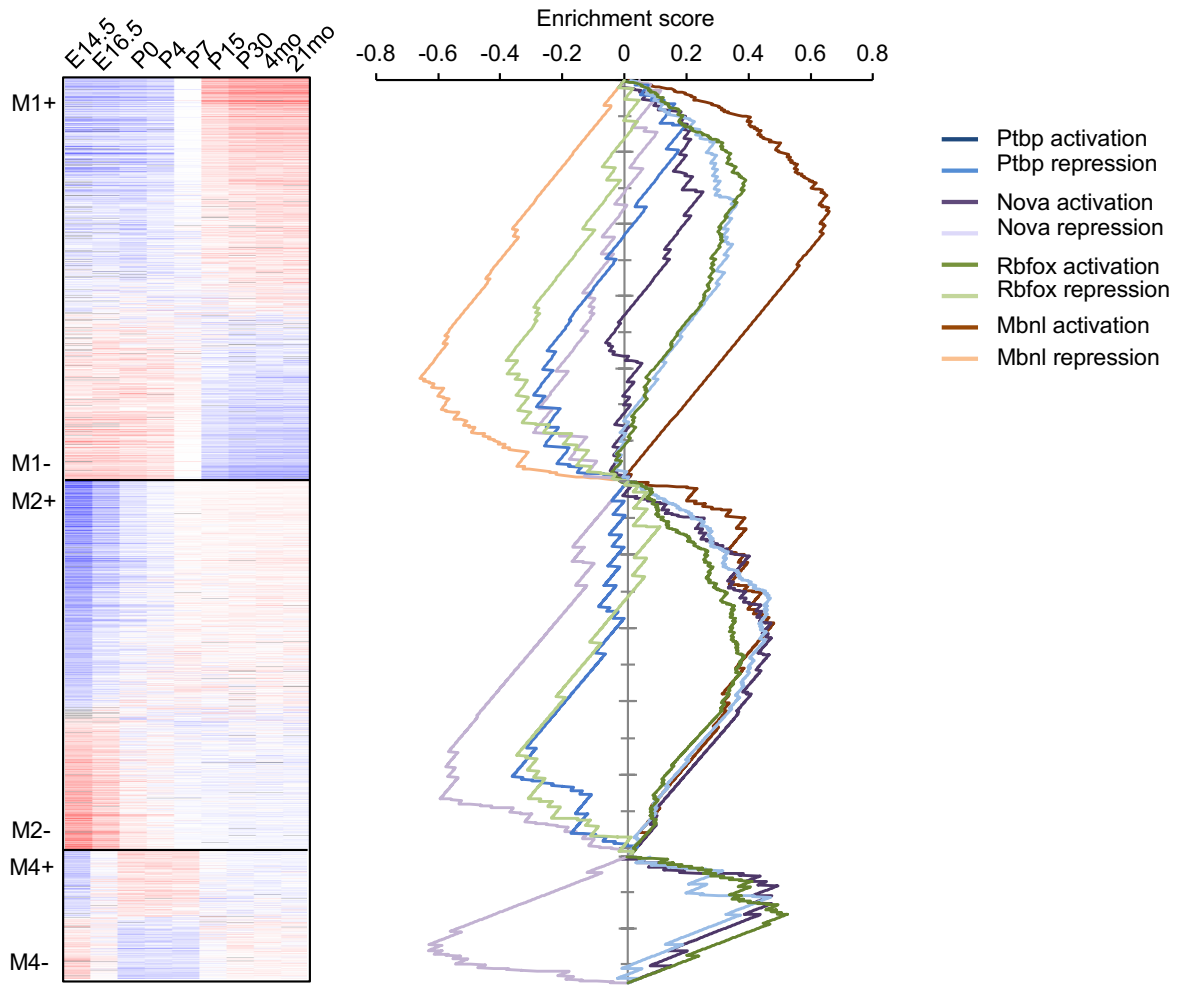


**Fig. S9. Gene Set Enrichment Analysis (GSEA) of RBP targets in WGCNA module exons.** GSEA was performed for exons in modules M1, M2 and M4 separately. Each gene set is defined by the group of target exons activated or repressed by specific RBPs.

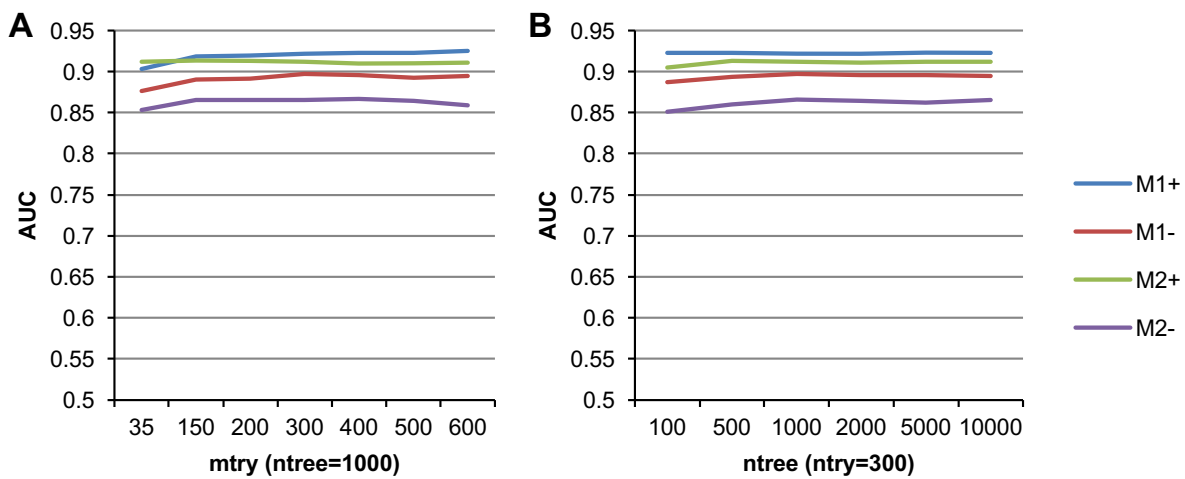


**Fig. S10. Performance of random forest in predicting module exons using different parameters. (A)** Performance vs. number of variables per tree in the forest (mtry). **(B)** Performance vs. number of trees in the forest (ntree).

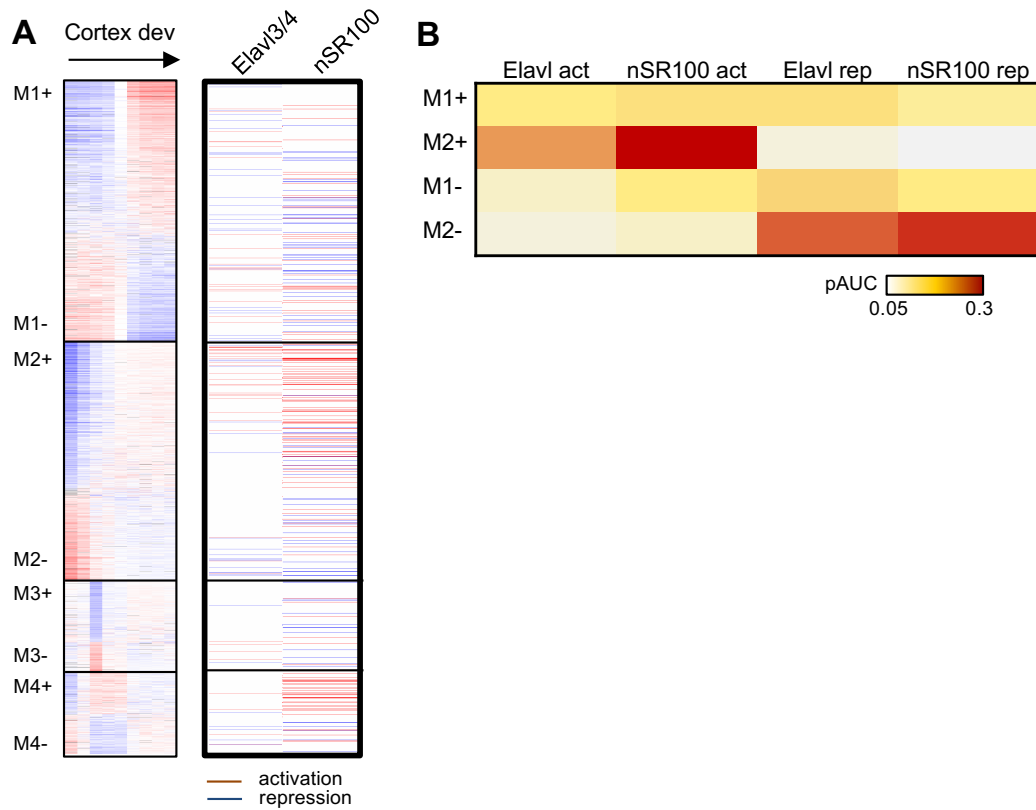


**Fig. S11. Additional neuronal RBPs contributing to early splicing switches.** **(A)** Activation or repression of module exons by Elavl3/4 and nSR100. Elavl3/4-dependent exons were identified by comparison of WT and Elavl3/4 dKO mouse cortices using exon-junction microarrays (Ince-Dunn et al.;  $|\Delta\text{IRank}| \geq 6.5$ ). nSR100 (SRRM4)-dependent exons were identified by comparison of WT and nSR100 KO mouse hippocampi using RNA-seq ( $|\Delta\Psi| \geq 0.1$ , Benjamini FDR  $\leq 0.05$ ). **(B)** Similar to Fig. 4J in the main text. Prediction performance of exon module membership based on regulation by each RBP family. Activation or repression by each RBP as determined from exon-junction microarrays or RNA-seq was used to predict early and late splicing switches, as well as the direction of switches. The performance is measured by partial area under curve (pAUC) of the receiver operating characteristic (ROC) plot with a cutoff at false positive rate (FPR)  $\leq 0.1$ .

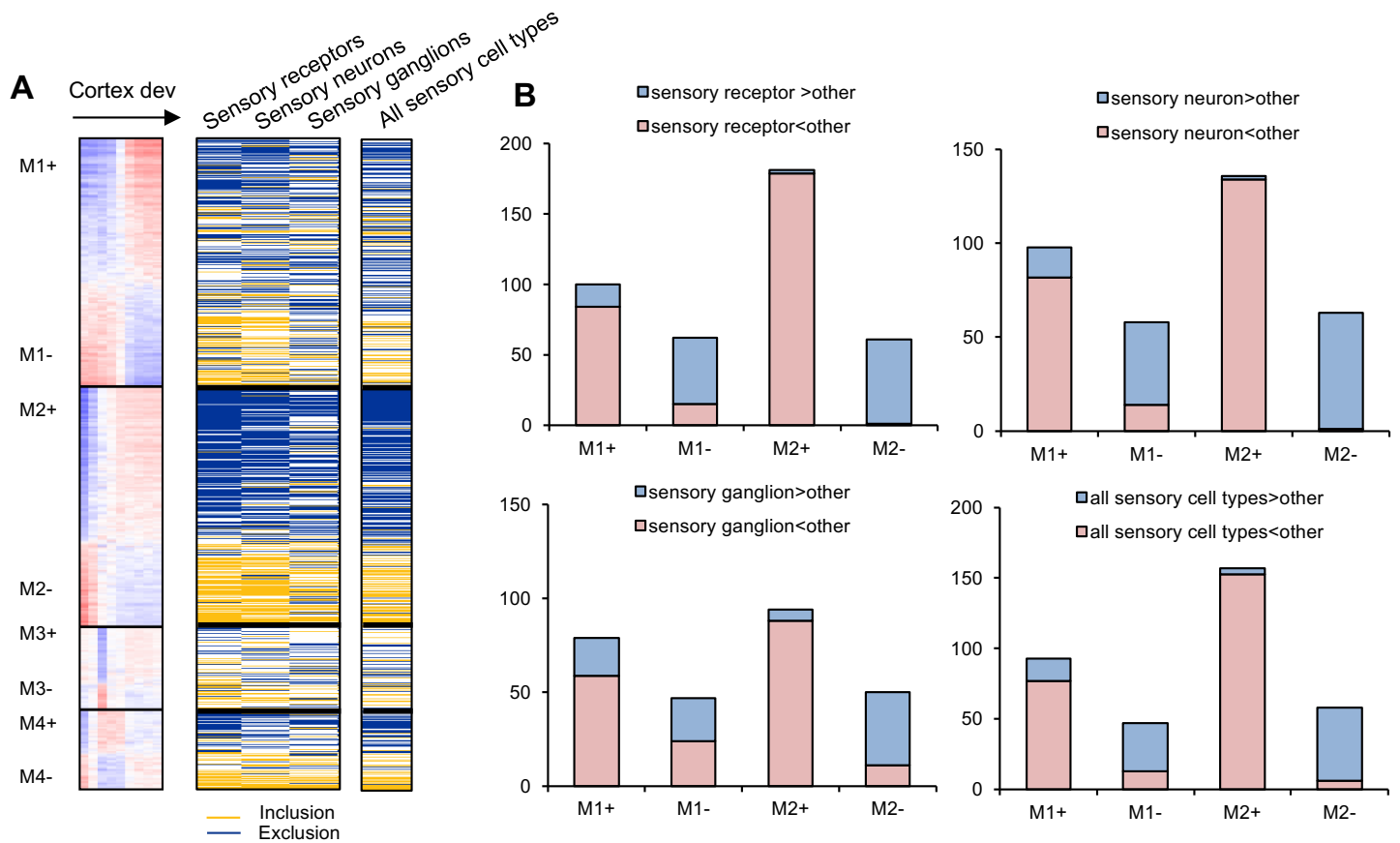


**Fig. S12. Differential splicing analysis of peripheral and sensory neurons compared to mature CNS neurons. (A)** Heatmap showing exons with statistically significant inclusion (yellow) and exclusion (blue) in each type of peripheral and sensory cells (sensory receptors, sensory neurons and sensory ganglion neurons) compared to the mature CNS neurons. **(B)** Overlap between core module exons and exons showing differential splicing in each type of peripheral sensory cells compared to mature CNS neurons. Exons with increased or decreased inclusion in each module and direction are shown separately.

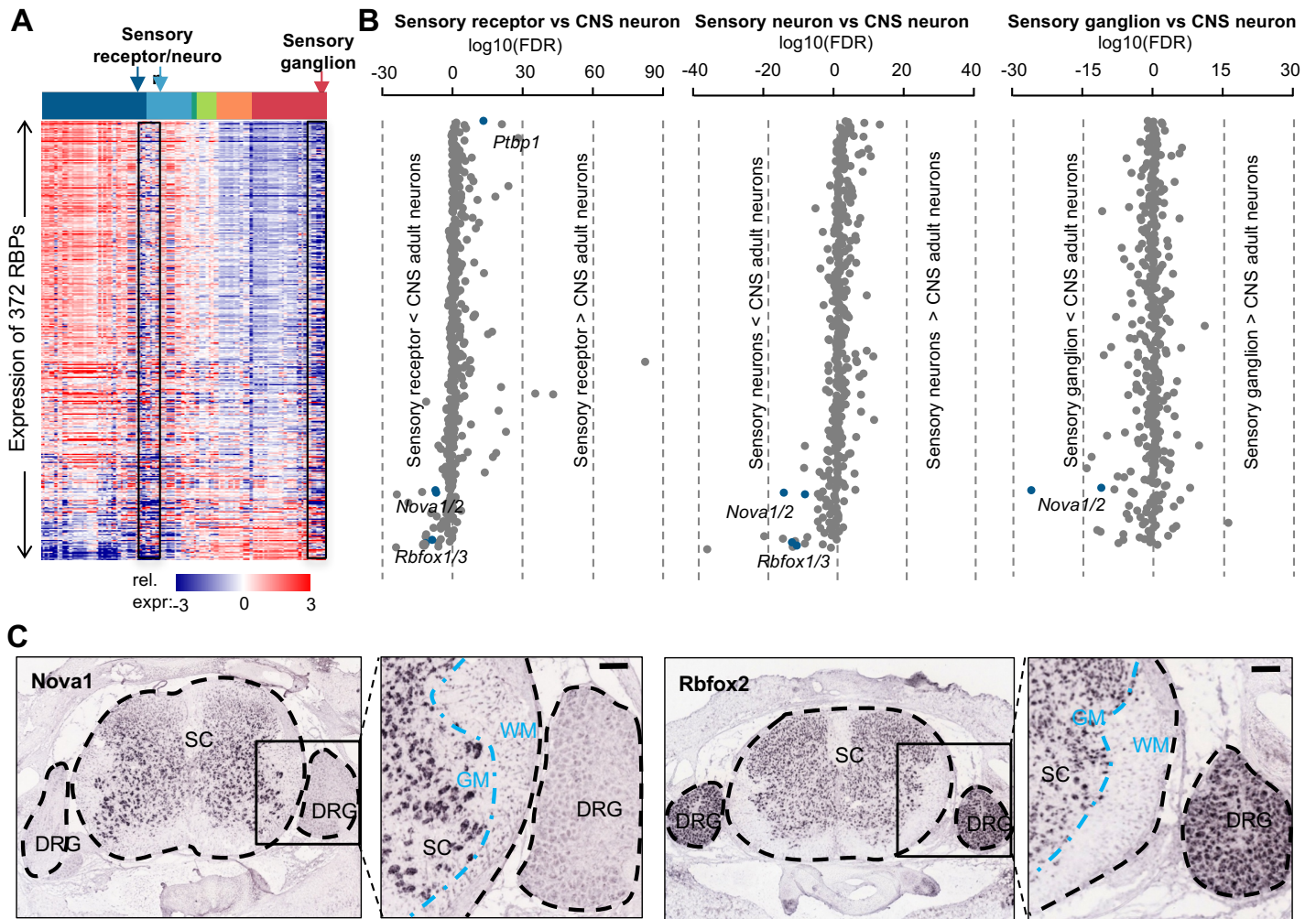


**Fig. S13. Only specific RBPs show distinct expression in peripheral and sensory neurons compared to mature CNS neurons. (A)** Expression of RBPs (log<sub>2</sub> transformed, median centered RPKM values) across different tissue or neuronal samples was used in the analysis. This analysis included all RBPs compiled in RBPDB (<http://rbpdb.ccb.utoronto.ca>). The same list of 346 samples used to predict maturation stages (table S1) was analyzed. Samples were ordered by the predicted maturation stage, and RBPs were ordered by the correlation of their expression with the predicted sample maturation stages. Sensory cell types are highlighted. The data matrix used to generate this heatmap is available in table S13. **(B)** Differential expression analysis of RBPs in each cell type from the peripheral and sensory system compared to mature CNS neurons purified from adult mouse brains. The Benjamini FDR (in log<sub>2</sub> scale) with sign indicating the direction of expression difference is shown. RBPs are shown in the same order as in (A). A subset of RBPs are highlighted. **(C)** *Nova1* (top) and *Rbfox2* (bottom) expression in P4 mouse spinal cord using in situ hybridization. Data were obtained from Allen Brain Atlas (<http://mousespinal.brain-map.org>). In the spinal cord, gray matter and white matter are indicated due to neuron-specific or enriched expression of *Nova* and *Rbfox2*. Probes for *Nova2* and *Rbfox1/3* are not available. SC, spinal cord; DRG, dorsal root ganglion; WM, white matter; GM, gray matter. Scale bar: 100  $\mu\text{m}$ .